

Thermische Eigenschaften eines hybriden Verbundwerkstoffs für Produktionsanwendungen in der Luft- und Raumfahrt

Thermal Properties of a Hybrid Composite Material for Aerospace Production Applications

María Fernández de Palencia Navarro

Scientific thesis to pursue the degree B.Sc.

Supervisor

Univ.-Prof. Dr.-Ing. Klaus Drechsler
Chair of Carbon Composites

Tutor

Matthias Feuchtgruber, M.Sc.
Chair of Carbon Composites

Submitted by

María Fernández de Palencia Navarro
Calle Císcar 59
46005 Valencia
Tel.: +34629603931
Matr.-Nr.: 03753744

Submitted on

19.09.2022 in Valencia

Technische Universität München
Fakultät für Luftfahrt, Raumfahrt und Geodäsie
Lehrstuhl für Carbon Composites
Boltzmannstraße 15
D-85748 Garching bei München

Tel.: +49 (0) 89 / 289 – 15092

Fax: +49 (0) 89 / 289 – 15097

Email: info@lcc.lrg.tum.de

Web: www.lrg.tum.de/lcc

TASK STATEMENT

Chair of Carbon Composites
TUM School of Engineering and Design
Technical University of Munich



Bachelor's Thesis, Term Project, Master's Thesis

Material Characterization of Novel Hybrid Composites

Additive Manufacturing by Material Extrusion– also known as 3D printing – uses thermoplastic polymers to create complex structures layer by layer. Automated Fibre Placement places tapes of continuous fibres according to a given path. The project at the chair will combine these two composite manufacturing technologies into an Advanced Tape Layer Additive Manufacturing (ATLAM) process. By the integration of continuous fibres, it is possible to achieve identical coefficients of thermal expansion as traditional composite parts possess. The ATLAM process will enable aerospace manufacturers to generate composite tools quick and cheap compared to the current state. Specifically, for the current project, landing flaps for an Airbus passenger aircraft shall be manufactured with the produced tools. The long-term goal is to manufacture flying structural parts for the aerospace industry.

The newly developed manufacturing process of the short fibre reinforced material and the continuous tape needs to be investigated for thermal behaviour to determine the material properties. Therefore, it is necessary to obtain conductivity and convection coefficients of the hybrid composite. The first work package will be a literature research on suitable test methods followed by the determination of the coefficients including the manufacturing of the samples. Depending on the type and focus of the thesis, the work packages will be adapted.

Research focus of the thesis

- Literature research: Thermal properties of CFRP
- Experimental set up
- Measurements
- Documentation

Requirements

- Clean and independent way of working
- Interest in material testing and composites
- Basic knowledge in test standards of composites is an advantage



Figure 1: 3D printed test cube

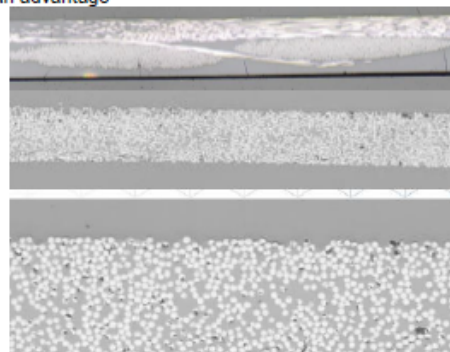


Figure 2: Microscopic image of the fiber distribution in the tapes between the 3D printed layers

Starting date: Now, flexible

For more details please contact:

Matthias Feuchtgruber, Room 5504.01.428, FSZ, Tel. +49 89 / 289 – 10385, matthias.feuchtgruber@tum.de

SWORN DECLARATION

Ich erkläre hiermit ehrenwörtlich, dass ich die vorliegende Arbeit selbstständig und ohne Benutzung anderer als der angegebenen Hilfsmittel angefertigt habe; die aus fremden Quellen (einschließlich elektronischer Quellen) direkt oder indirekt übernommenen Gedanken sind ausnahmslos als solche kenntlich gemacht.

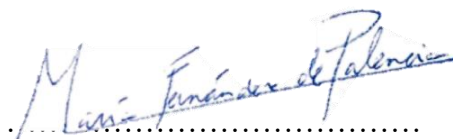
Die Arbeit wurde in gleicher oder ähnlicher Form noch keiner anderen Prüfungsbehörde vorgelegt.

I hereby declare that I have written this thesis independently and without the use of any other aids than those indicated; any thoughts taken directly or indirectly from external sources (including electronic resources) are identified as such without exception.

The thesis has not been submitted in the same or in a similar form to any other examination authority.

..... Valencia, 19.09.2022

Place, date

.....

Signature

ÜBERBLICK

Diese Arbeit beinhaltet eine Untersuchung der thermischen Eigenschaften eines kohlenstofffaserverstärkten Kunststoffs (20 % kurze Kohlenstofffasern und 80 % PEI) und der Materialeigenschaften, die diese Eigenschaften beeinflussen. Die Arbeit beinhaltet eine Literaturrecherche über Verbundwerkstoffe, Produktionsmethoden sowie Konvektions- und Konduktionsmessmethoden. Die Methodik zur Durchführung der Experimente sowie die daraus gewonnenen Ergebnisse werden in dieser Arbeit detailliert beschrieben. Am Lehrstuhl für Carbon Composites der TUM wurden mehrere Experimente zur Ermittlung des Wärmeleitfähigkeitskoeffizienten, der Ausbreitung des Wärmestroms und des Konvektionskoeffizienten durchgeführt. Erkenntnisse über die Auswirkungen der Faserrichtung auf die Ausbreitung des Wärmestroms, den Einfluss der Druckrichtung auf den Leitfähigkeitskoeffizienten und den Einfluss der Schwerkraft auf die Konvektion werden in diesem Projekt dargestellt.

ABSTRACT

This project contains a study of the thermal properties of a Carbon Fiber Reinforced Plastic composed (20% of short carbon fibers and 80% of PEI) and the material characteristics that influence them. The thesis contains a literature search over composite materials, production methods, and convection and conduction measurement methods. The methodology described to perform the experiments as well as the results obtained from them, is detailed in this paper. Multiple experiments for obtaining the conductivity coefficient, the propagation of the heat flow, and the convection coefficient were performed at the Chair of Carbon Composites of the TUM. Conclusions about the effects of the fiber direction on the propagation of the heat flow, the influence of the printing direction on the conductivity coefficient, and the influence of the gravity in the convection are found in this project.

INDEX

TASK STATEMENT	III
SWORN DECLARATION	IV
ÜBERBLICK.....	V
ABSTRACT	VI
INDEX.....	VII
NOMENCLATURE	IX
LIST OF ABBREVIATIONS.....	XII
1. Introduction	1
2. State of the art	3
2.1. Carbon Composite materials.....	3
2.1.1. Definition.....	3
2.1.2. Properties	5
2.1.3. Use cases for aerospace applications.....	6
2.2. Production processes of composites	7
2.2.1. Material extrusion technique: definition types and problems	8
2.3. Conductivity.....	9
2.3.1. Definition.....	9
2.3.2. Thermal conductivity characterization of composite materials.....	10
2.3.3. Methods for measuring conductivity coefficient.....	12
2.4. Convection	15
2.4.1. Definition.....	15
2.4.2. Methods for measuring convection coefficient	15
3. Method	19
3.1. Development of the test specimen	19
3.2. Measuring techniques	21
3.2.1. Conductivity	21
3.2.2. Convection.....	23
4. Results and discussion.....	27
4.1. Conductivity coefficient.....	27

4.1.1. Sample 1.....	28
4.1.2. Sample 2.....	31
4.1.3. Sample 3.....	34
4.1.4. Discussion of the conductivity results	34
4.2. Conduction and fiber alignment	35
4.2.1. Heat flow distribution at Sample 1	36
4.2.2. Study of the influence of fiber alignment	37
4.3. Convection.....	38
4.3.1. Rough sample.....	38
4.3.2. Smooth sample.....	40
4.3.3. Effect of the gravity: rough sample in vertical position.....	41
5. Summary and outlook	43
REFERENCES.....	45
LIST OF FIGURES.....	48
LIST OF TABLES	49

NOMENCLATURE

Formula symbol	Unit	Description
P	[W]	Electrical power
\dot{Q}	[W/m ²]	Heat flux density
R	[Ω]	Electrical resistance
U_{high}	[V]	Voltage amplitude
η	[-]	Efficiency
DC	[-]	Pulse duty factor
t	[s]	Time
λ	[W/m K]	Thermal conductivity
h	[W/m ² K]	Convection coefficient
K	[W/m K]	Thermal conductivity of the material
T	[K]	Temperature
dT/dx	[K/m]	Change in temperature across the thickness
Q	[W]	Quantity of heat
L	[m]	Unit thickness

X NOMENCLATURE

Formula symbol	Unit	Description
A	[m²]	Unit area
ΔT	[K]	Temperature gradient
κ_{TOT}	[W/m K]	Total thermal conductivity
P_{SAM}	[W]	Power flowing through the sample
L_S	[m]	Length between the thermocouples
P_{IN}	[W]	Input power
P_{LOSS}	[W]	Output power
D	[m²/s]	Thermal diffusivity
ρ_d	[kg/ m³]	Density
C_p	[J/kgK]	Heat capacity
T_s	[K]	Surface temperature
T_∞	[K]	Fluid bulk mean temperature Ambient temperature
δ	[m]	Boundary layer thickness
d	[m]	Sample thickness
b	[-]	Ratio between heat flow propagation in y direction over x direction

C_y	[px]	Length of heat flow propagation in y direction
C_x	[px]	Length of heat flow propagation in x direction

LIST OF ABBREVIATIONS

Abkürzung	Beschreibung
ABS	Acrylonitrile butadiene styrene
CFRP	Carbon fiber reinforced plastic
PEI	Polyetherimide
MEAM	Material Extrusion Additive Manufacturing
FFF	Fused Filament Fabrication
GFRP	Glass fiber reinforced polymer
PAN	Polyacrylonitrile
USB	Universal serial bus
PWM	Pulse width modulation
HTC	Heat transfer coefficient
ATLAM	Advanced Tape Laying Additive Manufacturing
AFP	Automated Fiber Placement

1.Introduction

Nowadays, composite materials are widely used in different engineering sectors due to their high-performance mechanical and thermal properties. With the selection of the proper matrix and fiber materials and the correct percentage of them, an optimization of their properties to fulfill the purpose of the material can be achieved.

As research into composite materials and their production methods have been developed, their use has increased in the aerospace sector. An example is the Boeing 787 (Dreamliner), in which the wings and the fuselage are made of carbon fiber/epoxy composites. [1]

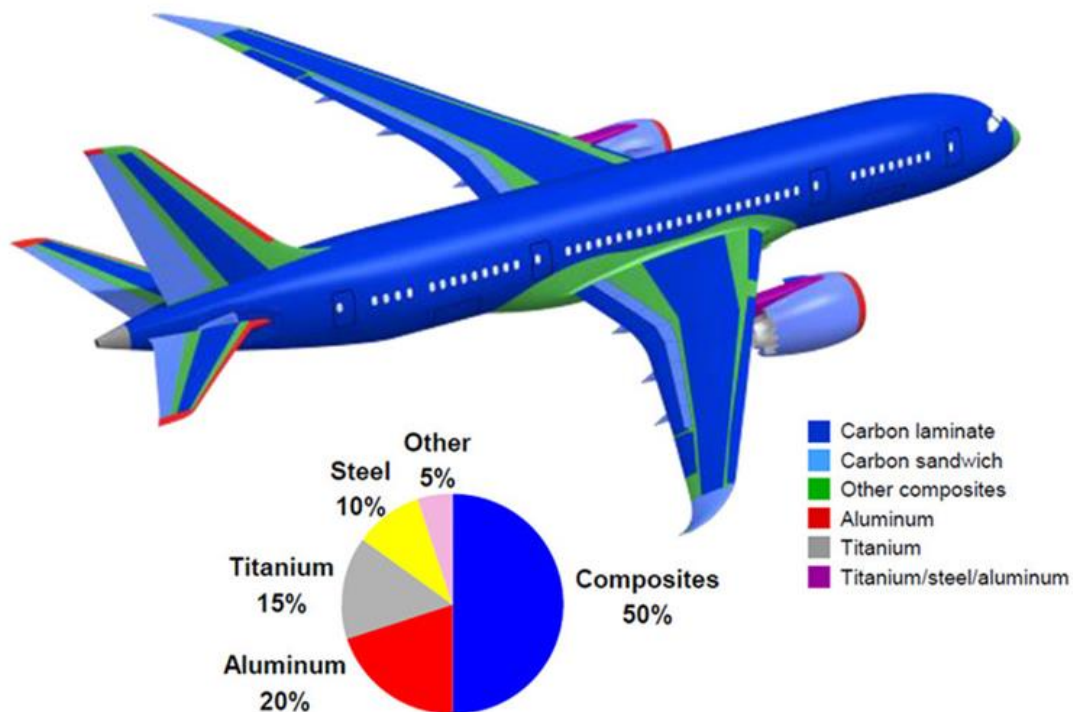


Fig. 1-1: " Composite structure content on the Boeing 787 [2]"

In the aerospace sector, carbon composites play an important role. Their high strength and their resistance to high temperatures makes them suitable for this application. An

2 Introduction

advantage is that their density is lower than the metal alloys that were more commonly used. The lower weight of carbon composites implies lower operation empty weight and less fuel is needed. Moreover, it also implies a technical upgrade as greater payloads can be carried, and longer ranges are also achievable. [1]

The Advanced Tape Layer Additive Manufacturing (ATLAM) process combines the 3D printing with the Automated Fiber Placement (AFP) that places tapes of continuous fibers according to a given path. By the integration of continuous fibers, it is possible to achieve identical coefficients of thermal expansion as traditional composite parts possess. With this process aerospace manufacturers will be able to generate compositetools quick and cheap compared to the current state. For the current project, landing flaps for an Airbus passenger aircraft shall be manufactured with the produced tools.

The 3D printing technique of Material Extrusion Additive Manufacturing (MEAM) is becoming more popular in the last years because it allows the manufacturing of pieces with complex geometries with good properties. The technique implies a cost and time reduction in autoclave tool manufacturing. The production efficiency and material properties can be improved by knowing the conduction and convection coefficients during the manufacturing process. [3,4]

For this purpose, this document contains research on composite materials' components and production methods and how they influence their thermal properties. Moreover, the definitions of thermal conductivity and convection can be found as well as the current methods for measuring them.

2. State of the art

This section discusses the current state of the art regarding carbon fibre reinforced composites and the thermal effects during the MEAM process.

2.1. Carbon Composite materials

2.1.1. Definition

A composite material combines two or more materials. Its two indispensable constituents are fiber reinforcement and the matrix. This combination upgrades the properties of the elements separately; nevertheless, the materials retain their original chemical, physical and mechanical properties. [1]

- **Reinforcement**

The reinforcement is usually harder, stronger, and stiffer than the matrix. It can be with fibers or particulates. [5]

Based on the laminate configuration the composites can be classified in unidirectional lamina (single or several laminas with the same material and orientation), laminate (several laminas stacked and bonded together but with different orientation or material) and bulk composites (laminas cannot be identified). [5]

Composites can have a hybrid structure if more than one material is used, different materials can be in various laminas or different reinforcements can be in the same lamina. [5]

Particulates and whiskers have equal dimensions in all directions. They present different geometries and typically are weaker and less stiff than continuous fiber composites. This type of reinforcement is cheaper than others. Their orientation can be random or preferential. [1,5]

In the case of fibers, the length is greater than the diameter, and the ratio between both is the aspect ratio of the fiber. Two types of fibers can be distinguished based on the aspect ratio: continuous fibers with long aspect ratios and discontinuous fibers with short aspect ratios. The first ones can present an unidirectional fiber orientation, a bidirectional fiber orientation or a random orientation while the discontinuous fibers present a random or preferential orientation. [1,5]

Fibers produce high-strength composites and can reduce defects in the composite compared to the matrix material by itself. It can be said that the smaller the diameter of the fiber, the more significant the strength and greater the flexibility; however, usually, this implies a higher cost. [1]

The typical fibers include glass, aramid, and carbon; the type and percentage of reinforcement determine the properties of the composite. [1]

- **Matrix**

It corresponds to the continuous phase and can be made of polymer, metal, or ceramic. The matrix performs several functions in the composite, such as maintaining the fibers in the proper orientation and spacing and protecting them from abrasion and the environment. [1]

There is a limit of a minimum of 30% of the matrix in a composite; a smaller percentage will result in an insufficient matrix to support the fibers effectively. [1]

Polymer matrices are differentiated in thermoset and thermoplastics. Thermosets result from an irreversible chemical transformation of the initial resin into an amorphous cross-linked polymer matrix. Thermoplastics are formed by adding polymerization and can be modified or reused [6]. Thermoplastics can be reheated once cured above their melting temperature for additional processing.

It is known that metallic and ceramic matrices present a much better thermal stability than polymeric matrices; however, their processing implies higher temperatures, pressures, and costs. [1]

In this project, a short carbon reinforced composite in a PEI (Polyetherimide) matrix will be employed. The percentages are 80% of PEI matrix and 20% of carbon fibers.

2.1.2. Properties

Carbon composites are widely used due to their advantages, such as their light weight, good strength, and stiffness properties, improved fatigue life, corrosion resistance, and reduced assembly cost, as fewer manufacturing parts are needed.

However, the use of composites also implies disadvantages such as increased costs in raw materials, high fabrication and production costs, and adverse effects of temperature and moisture. When the loads are applied out-of-plane direction, the strength of the composite decays significantly, being more likely to impact damage such as delaminations or ply separations. The reparation of the damages in composites implies more manufacturing difficulty than in other materials. Apart from loads other factors that can influence the mechanical properties are the temperature and the moisture.[1]

Thermal properties depend as well in the direction of the fiber orientation as well as in the properties of the fibers and the matrix. In the table Tab. 2-1 the thermal conductivity properties of the carbon fibers and the Polyetherimide (PEI) can be found.

Tab. 2-1: Matrix and fiber properties [7,8]

Property	Carbon	PEI
Density	1.79 g/cm ³	1.27 g/cm ³
Thermal conductivity	1.7 W/Km	0.24 W/Km

Taking into account the thermal conductivity of the matrix and fibers from the data sheets, the theoretical thermal conductivity of the composite material can be calculated by the rule of mixture.

$$\lambda = 0.24 \cdot 80\% + 1.7 \cdot 20\% = 0.532 \text{ W/Km} \quad (2-1)$$

More detailed information about the thermal properties of composites are found in the following sections.

2.1.3. Use cases for aerospace applications

The composites' applications include aerospace, transportation, construction, sporting goods, marine goods, and infrastructure. Their most significant presence is in the sectors of construction and transportation. [1]

Composites are widely used in aerospace production applications due to their excellent mechanical and thermal properties and their light weight, which translated into improved performance, greater payloads, longer ranges, and fuel saving in aerospace vehicles. Moreover, composites significantly reduce the amount of assembly labor and the number of required fasteners. [1]

For high-performance applications, costlier continuous-carbon-fiber composites are used to provide high strength and stiffness while a low weight is maintained. On the other hand when the weight is not that critical cheaper options, such as fiberglass composites, are employed. [1]

Due to a weight saving of around 15 to 25 percent composite materials are used in the aerospace industry, and the forecast is that in the next few years, more aerospace parts will be produced with these materials. The use of composite materials was for years related to military applications for performance and payload reasons as well in helicopters in which the glass fiber reinforced rotor blades improved fatigue resistance, nowadays they have been substituted by carbon fiber composites. Due to the investigation on carbon composites in the military sector of aerospace improvements in small and large commercial aircrafts were implemented obtaining a decrease on the weight and an increase of fuel performance. In future years, large amounts of high-performance composites will be used in Airbus and Boeing aircrafts, an example of this is the Boeing 787 (Dreamliner) in which the wings and the fuselage are made of carbon fiber/epoxy composites. [1]

But as said at the beginning of the chapter composites are not only used in the aerospace sectors, Formula 1 monocoque are mainly build from carbon fiber composites to reduce weight and in marine applications composites are widely used to minimize the effects of corrosion. [1]

2.2. Production processes of composites

Depending on the materials used to produce the matrix and the type and length of reinforcement different production processes can be applied. Each production process has its advantages and disadvantages, in the following image the different production processes for thermosets and thermoplastics can be observed Fig. 2-1.

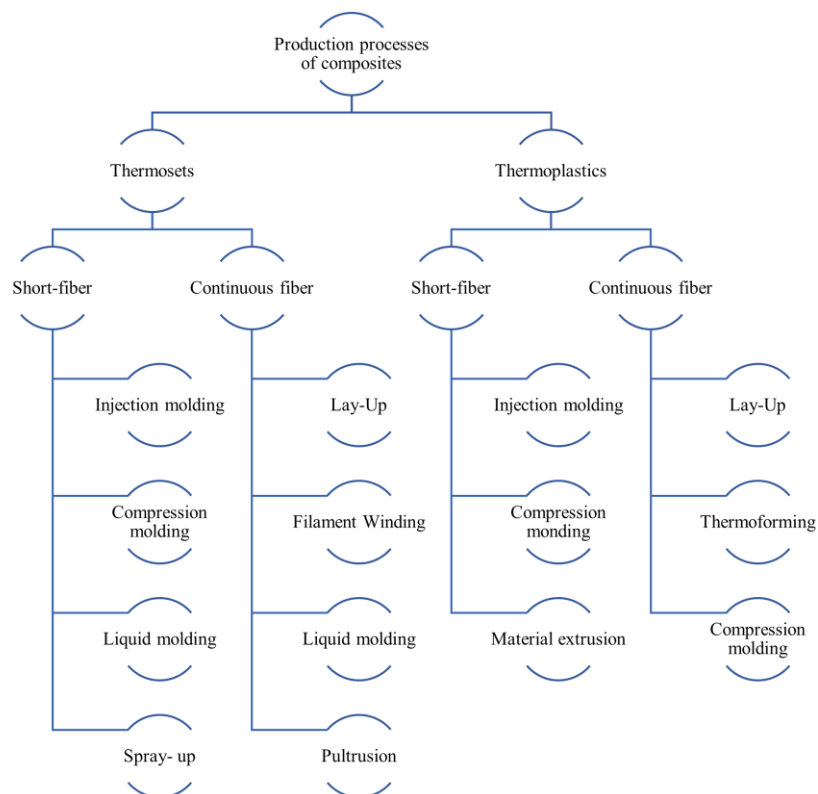


Fig. 2-1: "Production processes of composites adapted from [1]"

In the thermoplastic production, the main process variables are the time, the temperature, and the pressure. The production process is divided in the three stages heating, consolidation and cooling. The time required for the consolidation process depends on the heating method and the mass of the tooling. [1]

In terms of additive manufacturing processes two categories can be distinguished:

- The ones that use a thermal reaction bonding as state of fusion during production: material extrusion, material jetting and powder bed fusion.
- The ones that use a chemical reaction bonding as state of fusion during production: binder jetting, material jetting, var photopolymerization and sheet lamination. [4]

2.2.1. Material extrusion technique: definition types and problems

The technique of Material Extrusion Additive Manufacturing (MEAM), a subbranch of 3D printing, is becoming more popular in the last years as it allows the manufacturing of pieces with complex geometries with good properties. MEAM is also known as fused filament fabrication (FFF) in other scientific papers. [3,4]

The 3D printing technologies imply a cost reduction and time reduction in manufacturing. Other advantages are the design's freedom regardless of complexity and rapid iteration. [9]

Fiber reinforcement in 3D printing is widely used to improve the properties of polymers. In combination with carbon fibers, unique characteristics and capabilities are achieved. However, this technique is widely used in producing conceptual prototypes or for performing academic research and has not been implemented widely yet in the whole manufacturing market. [9,10]

In the filament fabrication process, the polymer is melted and extruded in a viscous or molten state through a nozzle to create a structure defined by a toolpath. After the deposition, the filament cools down and is solidified. Afterwards, the addition of new layers is allowed. [3,11]

The material extrusion technique allows direct manufacture complex structures that present more difficulty to produce with other methods with good properties such as their flexibility. However some drawbacks are found: [12]

- Lack of feedstock material that can compete with the high properties and functionality of the current engineering materials [12]
- The printing induces anisotropy and porosity in the parts [12]
- Lack of knowledge about the process-structure properties of the manufactured part. [12]
- The parts produced present poor mechanical properties compared to other methods such as thermoplastic injection [3]

One of the most significant compromises is finding adequate processing temperatures to achieve good adhesion. A high temperature is needed to develop a sufficient interface

healing of the filaments. At the same time, if the temperature is too high, it causes a low structure collapse due to low viscosity, thermal degradation, or chemical aging of the extruded polymer. [3]

In the filament scale, the mechanical properties decrease due to the macro-porosities inside the parts. The porosities in the material appear due to the circular shape of the filaments and the poor adhesion at the interface of adjacent filaments, these features are linked with the thermal history of the polymer. [3]

2.3. Conductivity

Conductivity measures of the hybrid composite material reinforced with carbon fibers are performed to understand the global thermal behavior.

2.3.1. Definition

In a material, the thermal conductivity (λ) represents the intrinsic property that relates the ability of the material to conduct heat. Conductive heat transfer involves the transfer of energy within a material without any motion of the material.

When a temperature gradient exists in a solid or stationary fluid medium, conduction occurs. Conductive heat flow follows the direction of decreasing temperature as the higher temperature corresponds to higher molecular energy and, therefore, more molecular movement. Energy is transferred from the more energetic to the less energetic molecules when adjacent molecules collide. [13]

According to Fourier's law of thermal conduction (2-2), for a homogeneous solid, the local heat flux is proportional to the negative local temperature gradient. The negative sign indicates the decrease in temperature from a hotter surface to a cooler surface. [14]

$$\dot{Q} = -K \frac{dT}{dx} \quad (2-2)$$

\dot{Q} : heat flux

K: thermal conductivity of the material

dT/dx: Change in temperature across the thickness

In equation (2-3) the thermal conductivity is defined as the quantity of heat transmitted per unit thickness in a direction normal to a surface of the unit area due to a unit temperature gradient under steady-state conditions and when the heat transfer depends only on the temperature gradient. [13]

$$\lambda = \frac{Q \cdot L}{A \cdot \Delta T} \quad (2-3)$$

λ : Conductivity

Q: Quantity of heat

L: Unit thickness

A: Unit area

ΔT : Temperature gradient

2.3.2. Thermal conductivity characterization of composite materials

The literature reveals that the conductivity properties, as well as other thermal properties and mechanical properties, depend on the fibers' orientation. In other words, composites present an anisotropic nature. Nevertheless, most composites can be considered orthotropic; only nine constants are required to describe them. [14]

The thermal conductivity of composites depends mainly on the properties of the fiber and the matrix.

2.3.2.1. Fibers

The manufactured composite's conductivity properties vary depending on the material used for the fibers. For example, glass fiber reinforced polymer (GFRP) presents similar

conductivity properties in any fiber direction, while the natural fibers act as insulators and present less thermal conductivity than the GFPR. [15]

In the carbon fibers used in this project, it can be observed that they are mainly produced using precursor materials (rayon, petroleum, or coal tar pitches and polyacrylonitrile or PAN) [15]. Multiple manufacturing techniques were involved to transform these precursor materials into carbon fibers. Spinning, stabilization to thermoset the fiber, carbonization, graphitization, surface treatment, and sizing are found in the techniques that can be employed. [16].

With the graphitization process at higher temperatures, properly ordered and oriented crystallites along the axis direction of the fiber is obtained. During this stage, for PAN-based carbon fibers, the linear structure of carbon atoms is transformed into a planar structure (basal planes) and are oriented or stacked along the axis of the fiber. Due to closely packed disposition of the basal planes, an increase in the electrical and thermal conductivities along the axis of the fibers occurs. [14]

The heat flow control can be more easily controlled when there is an alignment of the fibers and the printing direction. Fibers arranged orthogonal to the direction of the heat flow play a minimal role in the effective thermal conductivity in this direction, while when they are parallel to the heat flow, the effective thermal conductivity is more sensitive to the fiber volume fraction. That's to say, if two samples are composed of the same matrix and the same percentage of carbon fibers, the conductivity value will be higher in the one in which the fiber orientation is aligned with the heat flow. [17]

2.3.2.2. Resins

There are different options when talking about materials for matrix production. The most used ones are the metal, ceramic and polymer matrices. Polymer matrices are widely used because of their convenient properties at room temperature and their low-cost efficiency, as well as the facilities that they present when producing complex parts. [6]

There are two types of polymer matrices: thermoplastics and thermosets. Thermosets are the result of an irreversible chemical transformation of the initial resin into an amorphous cross-linked polymer matrix. They present good electrical and thermal insulation due to their large molecular structures. [6]

About thermoplastics, the matrix material that has been used for this project, they are formed by the addition of polymerization and can be modified or reused. They soften or fuse when heated and harden and become rigid after cooling. [6]

2.3.3. Methods for measuring conductivity coefficient

The selection technique for measuring the conductivity coefficient of the material depends on the configuration of the material and its future applications. Some of the possible techniques are:

- **Guarded heat flow meter (Steady-state method or absolute method):** The temperature difference across the sample is measured in response to the applied amount of heating power. For this method, a uniform heat flow must be provided to the sample, and a stable temperature for the measurements is required. If thermal conductivity is the only thermal property being measured, heat loss due to convection or conduction via the gas medium could cause differences in the measurements. [18]

The method follows the formula (2-4) in which:

$$\kappa_{TOT} = \frac{P_{SAM} \cdot L_S}{A \cdot \Delta T} \quad (2-4)$$

κ_{TOT} : Total thermal conductivity

P_{SAM} : power flowing through the sample

L_S : length between the thermocouples

ΔT : temperature variance

A : cross-sectional area of the sample where the power flows

For obtaining P_{SAM} , the difference between the input power (P_{IN}) and the power lost to radiation, heat conduction through gases, or the connection leads; or losses due to heat convection currents (P_{LOSS}) must be calculated (2-5). (2-5)

$$P_{SAM} = P_{IN} - P_{LOSS} \quad (2-5)$$

The image Fig. 2-2 is a visual representation of the simplified setup for this measurement technique. Inside the guard, the hot plate, the insulated sample, and the cold plate can be found. The sensors are found in the hot and the cold plate.

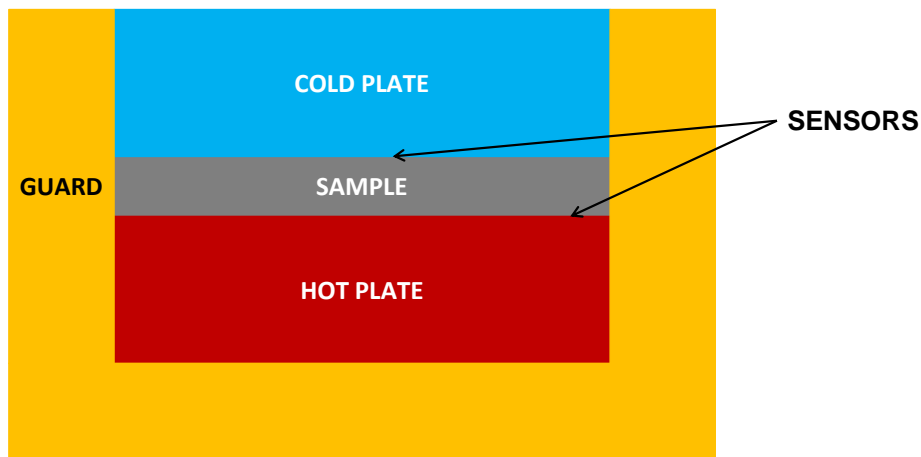


Fig. 2-2: Guarded heat flow mechanism

Numerous authors use thermocouples for thermal conductivity measurements. Only two wires of low thermal-conductivity material are required in this case to minimize the losses due to heat conduction. If wires are fixed with varnish or another adhesive for faster sample throughput, some advantages appear, but an error in the reading of the temperature variation also occurs. Another source of error can be calibration and subtraction of the lead contributions at low temperatures. [18]

Other heat losses can occur due to convection, circulating gas flow through the sample, or heat conduction. Minimizing these errors, arriving at a properly thermal anchoring, and adequately determining the cross-sectional sample length and the cross-sectional area, the higher precision that can be achieved will be a 5-10% uncertainty. [18]

- **Transient pulse method:** In this method, the dissipation of the thermal system is measured by an electrical model. Pulse heat responses are detected with a thermal physical tester. [14]
- **Flash pulse measurement:** In this direct method, the off thermal conductivity of a composite is measured. The composite sample is exposed to a pulse of radiant

energy, and measuring the travel time of this pulse through the section, the thermal diffusivity is calculated. [14]

- **Surface probe method or Mathis probe:** Is a non-intrusive indirect method with which the thermal conductivity of a heat flux parallel to the plane of a shape can be obtained. Three parallel nickel ribbons connected to an electrical circuitry provide a constant rate of heating to the sample and force the heat flux vector to be perpendicular to the probe surface. [14]
- **Radial flow method:** In this method, the errors due to the radiative losses at high temperatures from the heater and the sample surface are considered. These losses are minimized by applying the heat internally to the sample. It is generally used in solids with a wide range of thermal conductivities and are not commonly employed below room temperature. Its application is more complex than other linear flow methods. [18]
- **Laser-flash diffusivity:** On one side, the sample is irradiated by a short laser pulse, while on the other side of the sample, an IR detector monitors the rising temperature. The thermal diffusivity is calculated (temperature rise versus time profile) and is related to the conductivity by the formula (2-6), in which ρ_d is the density and C_p is the heat capacity. [18]

$$D = \frac{\kappa}{\rho_d C_p} \tag{2-6}$$

- **The pulse-power method ("Maldonado" technique):** Used for the first time by Maldonado in 1992 for measuring the heat conductivity and the thermoelectric power simultaneously, this method avoids the long waiting times between the measurements to reach the steady-state. A heater current generates a thermal gradient pulsed with a squared wave while the bath temperature is slowly drifted. This squared wave allows the creation of small thermal gradients. [18]

2.4. Convection

Convection measures of the hybrid composite material reinforced with carbon fibers are performed to understand the global thermal behaviour.

2.4.1. Definition

Convection or convective heat transfer corresponds to the heat transport processes affected by the flow of fluids [20]

The heat transfer coefficient (HTC) or convective heat transfer is used for calculating the heat transfer between a surface and a fluid moving, it can be expressed with the following formula (2-7) : [21]

$$h = \frac{\dot{Q}}{T_s - T_\infty} \quad (2-7)$$

Where:

h: heat transfer coefficient

T_s : surface temperature

T_∞ : fluid bulk mean temperature

\dot{Q} : surface/fluid interface heat flux (W/m^2)

2.4.2. Methods for measuring convection coefficient

The selection technique for measuring the convection coefficient of the material depends mainly on the conditions (internal and external) surrounding the experiment. Some of the possible techniques are:

- **Direct method:** This method is applied when a direct temperature and heat flux measurement can be performed. There are multiple options to measure the temperatures and the heat flux. In the table, different technique options for plates are found. [21]

Tab. 2-2: Direct method convection techniques [21]

Convection mode	Temperature/heat flux technique	Application
Gas free convection	Thermocouple/ interferometry Thermocouple/ heat flux sensor	Vertical flat plate, air Building wall, air
Liquid free convection	Thermocouple/interferometry	Supercooled water, flat plate
Nucleated boiling	Infrared/ Joule effect	Flat horizontal surface, water

The table shows that thermocouples are the most employed technique to measure the temperature directly at a solid. Other methods can be employed to measure the convection of different materials states.

- **Transient method:** This method is used when unsteady boundary conditions or non-equilibrium initial conditions are applied. The time constant or phase lag under thermal or boundary conditions is measured. A mathematical model of the transient response is developed to reduce the error with the experimental data. [21]
- **Wilson's method:** This method is employed to determine the heat transfer coefficient when there is more than one heat transfer process. It does not require direct measurements of the temperature; it only requires measurements of the fluid bulk. With the help of a second variable phase flow, the heat flux is imposed and the thermal resistance associated with the primary convection flow can be determined. [21–23]

- **Heat/momentum/mass transfer analogy method:** An analogy among heat, mass, and momentum transfer process is established for convective problems, and the measurements of this analogy are transferred into the original experiments since the results or both are alike. [21,24,25].
- **Boundary layer thickness method:** The thermal boundary layer thickness determines the local heat transfer coefficient. The heat can transverse the boundary layer by diffusive transfer (conduction) or advective transfer (bulk mass-energy transfer). The relationship between the local heat transfer coefficient and the boundary layer thickness follows the expression **(2-8)**. [21]

$$h(\delta) = \frac{k}{\delta}$$

(2-8)

- **Integrated HTC probes method:** By means of a probe, any of the previous methods described before is employed to obtain the heat transfer coefficient with a single coefficient. The most common integrated methods are the direct and the transient method employing a small sensor in regions where the small probe can be installed. [21]

3. Method

3.1. Development of the test specimen

The samples were produced by additive manufacturing with the material extrusion technique. The machine employed was a CEAD AM Flexbot, and as stated in previous sections, the composite PEI Airtech I-350CF is composed of 80% PEI and 20% short carbon fibers. In the picture, Fig. 3-1 the printing process can be observed. The printing bed has a rough surface ensuring adhesion of the composite to the surface and that the material does not expand to the sides.

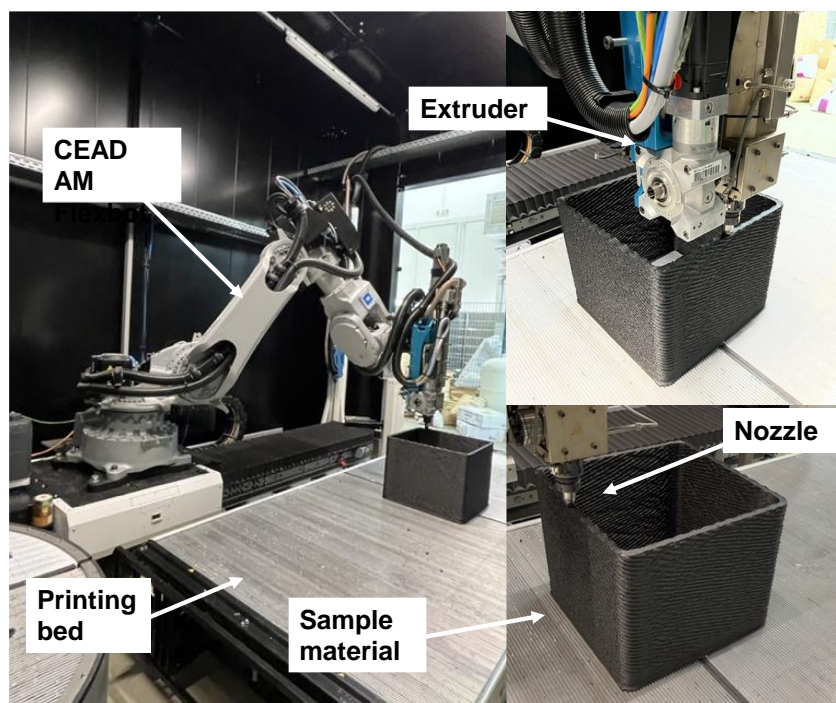


Fig. 3-1: Material extrusion

After this step, the samples to be studied on the test bench were cut into squares of approximately 10x10 mm to fit on the test bench. The machine employed for this was a Holzcraft HBS 533 (see Fig. 3-2). Some of the samples were polished for the experiments that needed a smooth surface (conductivity experiments and one of the convection experiments).



Fig. 3-2: Cutting machine

To measure the heat flow along the samples, they were drilled with a 5.9 mm diameter drill to fit tight the heat cartridge. The sharps of the holes were polished to avoid cuts (see Fig. 3-3).



Fig. 3-3: Drilling process

3.2. Measuring techniques

3.2.1. Conductivity

The characterization will be performed employing the machine developed by Michael Grünfelder that can be found at the Chair of Carbon Composites at TUM. [19]

The method described in the semester thesis is the Guarded heat flow meter described in the last subsection.

The following image Fig. 3-4, shows the setup of the guarded heat flow meter. The machine is connected to a laptop employing a USB cable; an Arduino code is implemented on the machine to obtain the following data:

- Elapsed time since the experiment began
- The temperature of the cold plate at the edge
- The temperature of the cold plate in the center
- The temperature of the hot plate
- The temperature of the guard
- Ambient temperature
- PWM (Pulse width modulation) is transferred to reach a stationary of a specific temperature

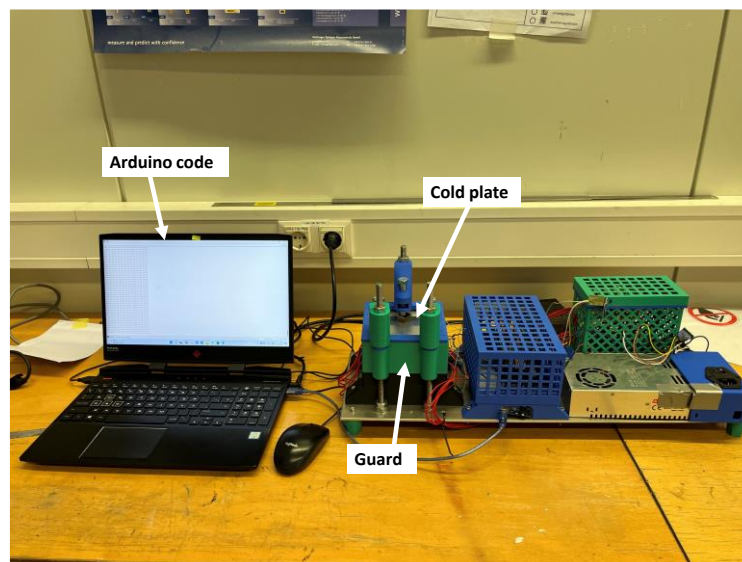


Fig. 3-4: Guarded heat flow meter at the TUM Chair of Carbon Composites

For calculating the thermal conductivity, the hot plate will be heated to a specific temperature. For the experiment, 60°C, 80°C, and 100°C were selected for the measurements. For obtaining the data, a steady-state is required. This will be achieved when the temperature of the hot plate and the temperature of the guards are both constant (taking into account some margins), and the PWM value is also constant.

Three samples of PEI Airtech I-350CF are selected for conducting the experiments:

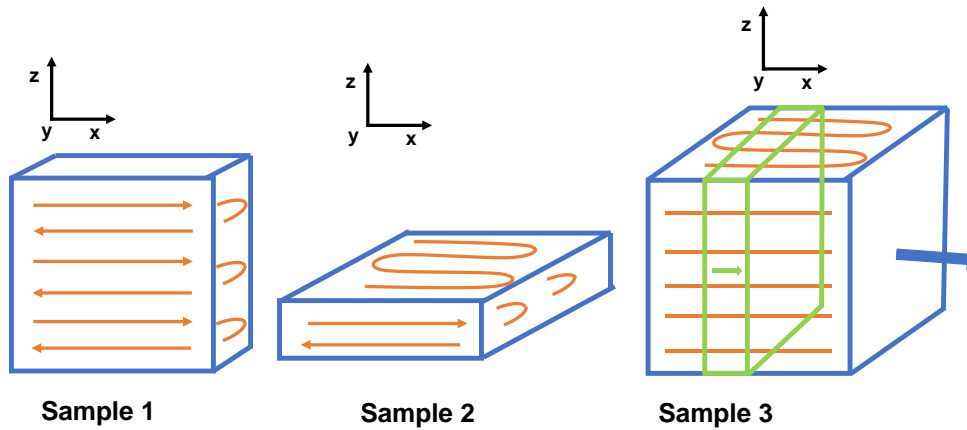


Fig. 3-5: PEI Airtech 1350 samples printing direction

Sample 1 and 2 printing directions are orthogonal to the heat flow while sample 3 printing direction is parallel to it. In sample 1 the layers are stacked one over the other in Z direction while in sample 2 the layers were placed one next to the other.

The data extracted with the Arduino code will be stored and processed in an excel file. Only the data for steady-state periods will be used for the calculations. The formula (3-1) is used for the calculation of the conductivity coefficient. [19]

$$\lambda = \eta \cdot \frac{U_{high}^2}{R} \cdot DC \cdot \frac{d}{\Delta T \cdot A} \quad (3-1)$$

3.2.2. Convection

The characterization will be performed by the same machine mentioned before

The method described in the semester thesis is based in the direct method described in the last subsection.

In order to measure the heat transfer coefficient the cool plate is taken out of the machine, so the carbon composite is exposed to the ambient air. Some pressure is implemented in the sample by means of the screws of the machine. In the image Fig. 3-6 it can be observed a scheme of the machine employed for the convection measurement.

For measuring the temperature of the surface a thermal camera (FLIR a235sc) was employed as well as the program FLIR Tools. The required temperature of the hot plate is set by an Arduino controller, a steady state will be considered reached once this temperature is reached and the value of the PMW is mainly constant for 10 minutes.

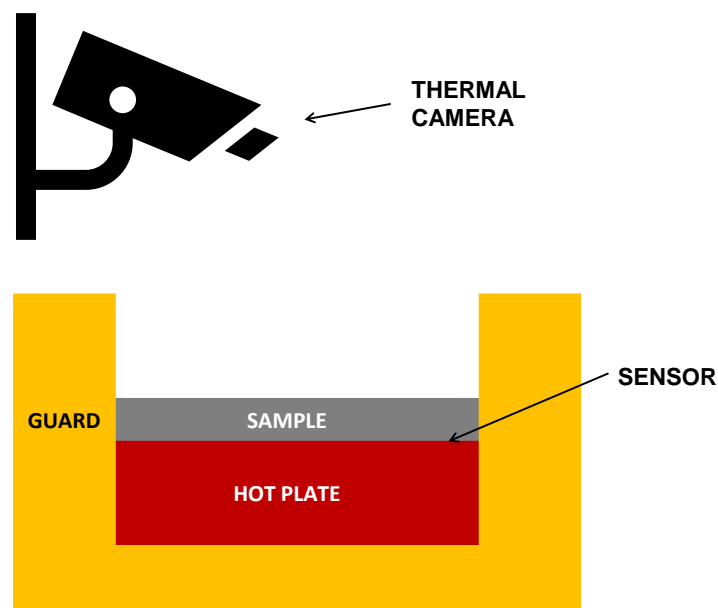


Fig. 3-6: Convection measurement

The heat flux at the surface is supposed to be constant assuming a steady state and the heat flux caused by conduction is equal to the one caused by convection $\dot{Q}_{\text{conduction}} = \dot{Q}_{\text{convection}}$. [19]

From the equation (3-2) assuming the steady state the equation (3-3) is obtained for calculating the convection coefficient

$$\frac{dT}{dx} = -\frac{h}{\lambda} \cdot (T_{\infty} - T_s) \quad (3-2)$$

$$h = \frac{\lambda}{d} \cdot \frac{\Delta T}{(T_s - T_{\infty})} \quad (3-3)$$

For the thermal conductivity λ the theoretical data calculated in the last subsection will be employed. The variation T , ΔT , is calculated by the subtraction of the temperature of the hot plate (measured by the thermocouple) minus T_s , temperature of the surface, (measured by the thermal camera). The ambient temperature is obtained with the external thermocouple of the machine. [19]

Three different measurements will be performed:

- One with the same sample 1 smoothed as in the conductivity measurements
- One with a sample with the same printing direction as the sample one but with a rough surface
- One with the machine tilted 90° with the last sample to see the gravitational effects on the convection coefficient and the distribution of the temperature along the sample.

On the following image Fig. 3-7 the layout of the test bench for the two first samples is shown.

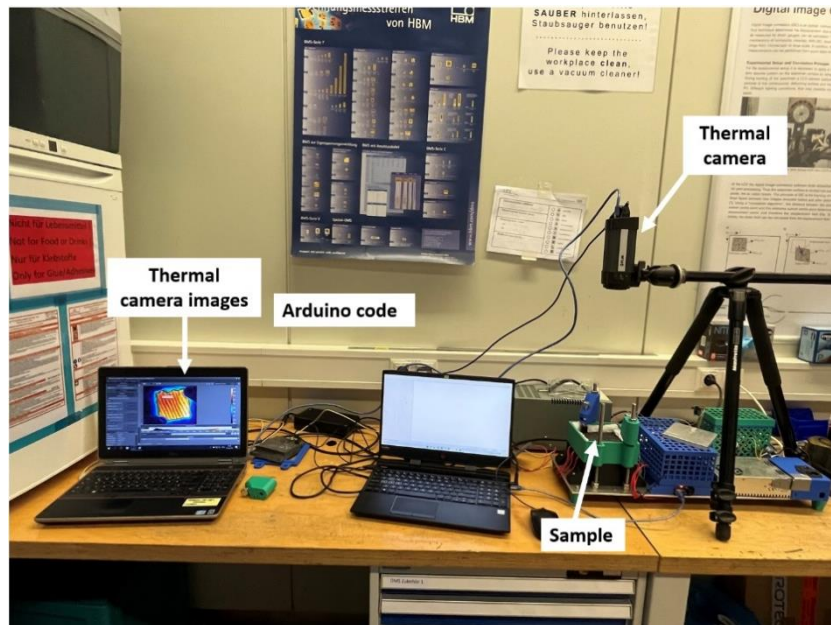


Fig. 3-7: Test bench for convection measurements

4. Results and discussion

In this chapter an analysis of the measurements obtained from the experiments is found. An analysis of the reliability and accuracy of the results will be performed as well as a selection of the validity of the results.

4.1. Conductivity coefficient

As mentioned in the above section, "Conduction: Technique selection," three samples were analyzed to obtain the conduction coefficient. As observed in the image Fig. 4-1, sample 1 and sample 2 result in the same printing direction (orthogonal to the heat flow), while the direction changes in sample 3 (parallel to the heat flow).

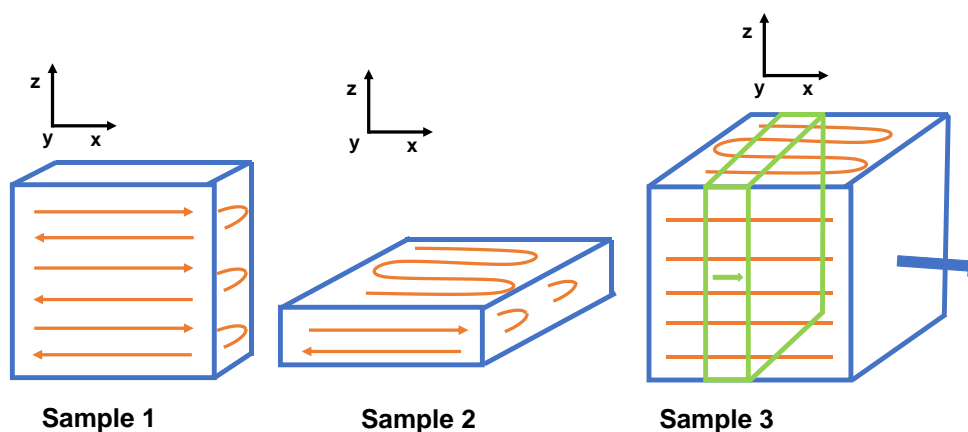


Fig. 4-1: PEI Airtech 1350 samples printing direction

In the "State of the art," the theoretical value of the conductivity coefficient was calculated, obtaining 0.532 W/mK. In the following subsections, the results will be compared with this value.

A numerical analysis will be performed using sample 1 to calculate the accuracy of the guarded heat flow meter machine.

For every sample experiment, 3 measurements at 60°C, 80°C and 100°C are performed to obtain the conductivity coefficient at those temperatures in a stationary state.

4.1.1. Sample 1

For sample 1, the printing direction was orthogonal to the direction of the heat flow. Three experiments with three measurements each were performed with the same sample to study the reliability of the data. In table Tab. 4-1 the different values of λ for each experiment can be observed.

The results of experiments 1 and 3 are most alike, while the results from experiment 2 deviate more from the average. The variance shows a slight deviation from the data set to the mean value.

It can be observed that the result closer to the theoretical value of the conductivity is at 100°C temperature. The mean value of conductivity is 0.40638 W/mK, while the theoretical value is 0.532 W/mK. This corresponds to a percentage difference of 23.61%.

Tab. 4-1: Conductivity coefficient of Sample 1, average and variance

	λ at T= 60°C	λ at T= 80°C	λ at T= 100°C
Sample 1_1	0.34348	0.38643	0.43246
Sample 1_2	0.26778	0.32971	0.36506
Sample 1_3	0.34857	0.39838	0.42162
Average	0.31994	0.37151	0.40638
Variance	0.00136	0.00090	0.00087

In the graph of the picture Fig. 4-2, it can be observed clearly how the measurements are performed. The heat plate is heated till reaching the set value, followed by the cold plate. The temperature of the guard reaches values like the heat plate values; however, it needs more time to reach a stationary set of values. The center of the cold plate is constantly rising its temperature.

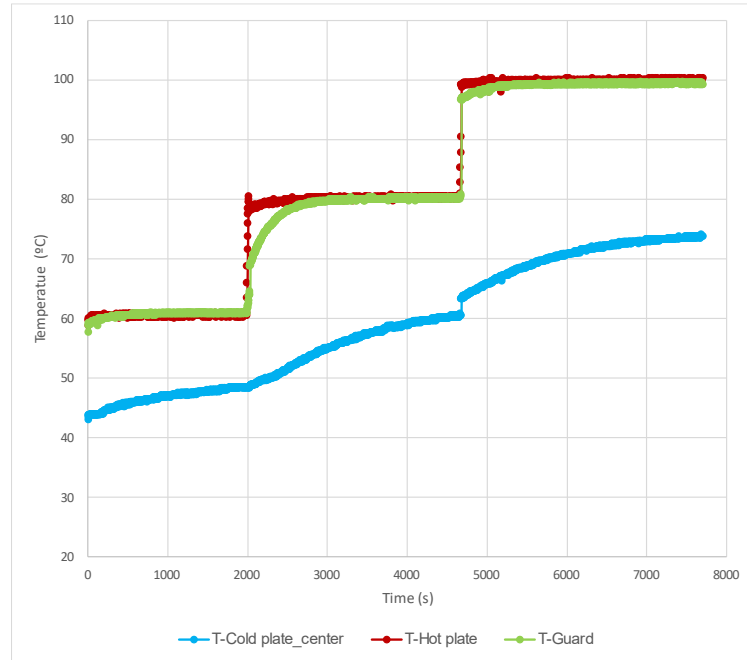


Fig. 4-2: Measurements Sample 1_1

For the second measurement (Fig. 4-3), it can be observed that the data is not recorded for around 40 minutes while the hot plate is at 100°C. Even though the data is not recorded during that period, the heat plate is still on. When the data started recording again, the temperature of the cold plate had raised.

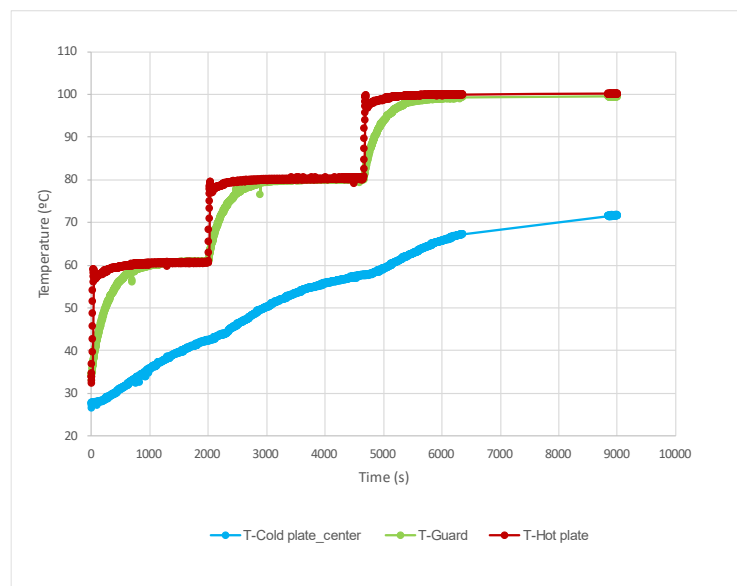


Fig. 4-3: Measurements Sample 1_2

For the third measurement (Fig. 4-4) the same problem of the data lack during certain periods of time is observed. Moreover, it can be observed that around 3500 seconds, there

is an error on the thermocouple temperature reading as the value does not fit any of their surrounding measurements.

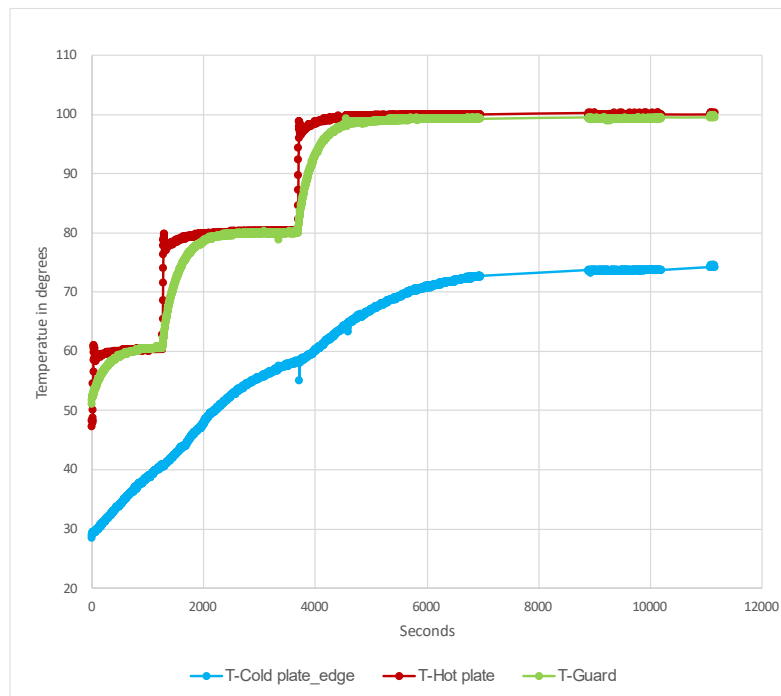


Fig. 4-4: Measurements Sample 1_3

There is an error regarding the theoretical data, but the measurements could be considered acceptable as their variance is small.

The machine cannot be considered accurate for the measurements due to the disconnection of data recording and because the cables were adjusted before every measurement to avoid misreading in the thermocouples.

The following graph (Fig. 4-5) shows how the temperatures recorded were unrealistic, arriving at minus zero temperatures. Moreover, some data from the hot plate was missing leaving gaps in those measurements. After this first attempt, the machine was repaired, and experiments 1,2, and 3 were performed. This malfunction of the machine and low accuracy of the thermocouples leads to conclude that the data that will be presented from these measurements is unreliable. Because of this, the theoretical conductivity coefficient will be used to calculate the convection coefficient.

Another reason for employing the theoretical conductivity coefficient is because as stated in the “State of the art” even minimizing the errors the higher precision that can be achieved with the guarded heat flow method is a 5-10% uncertainty. [18]

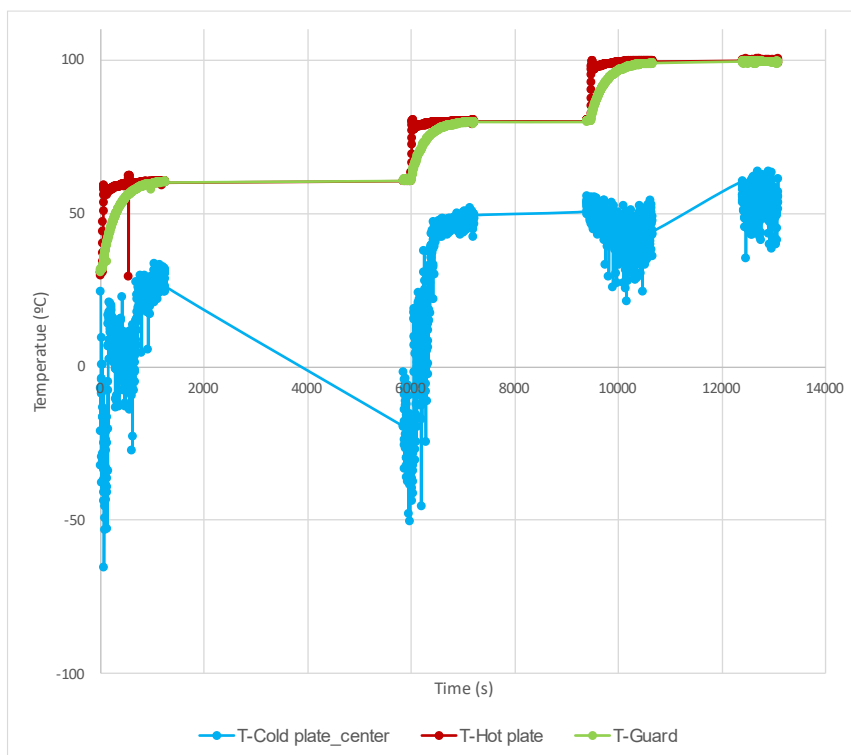


Fig. 4-5: Measurements Sample 1_0

4.1.2. Sample 2

For sample 2, similar results as sample 1 were expected as both samples have their printing directions orthogonal to the heat flow. However, some values in the conductivity coefficient were expected as in sample 1, the layers are stacked one over the other, while in sample 2 the layers were placed one next to the other.

The two experiments performed in sample 2 present significant variances confirming the hypothesis of the inaccuracy of the machine.

Tab. 4-2: Conductivity coefficient of Sample 2, average and variance

	λ at T= 60°C	λ at T= 80°C	λ at T= 100°C
Sample 2_1	0.21088	0.24337	0.22864
Sample 2_2	0.32841	0.33589	0.32951
Average	0.26964	0.28963	0.27907
Variance	0.00345	0.00214	0.00254

Table Tab. 4-2 shows the values obtained for sample 2. The tendency observed for sample 1 to increase the conductivity coefficient while the temperature is raised is not observed for sample 2. In sample 2, the conductivity coefficient increases between 60°C and 80°C but decreases again at T=100°C. Moreover, the variance between the two experiments increases in the order of magnitude with respect to the variance obtained for sample 1.

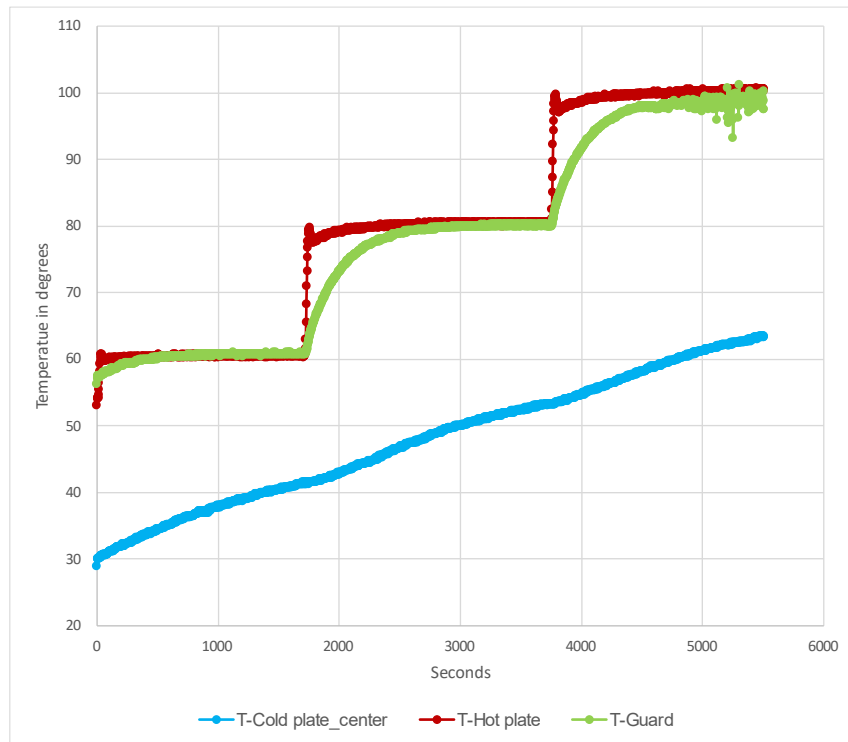
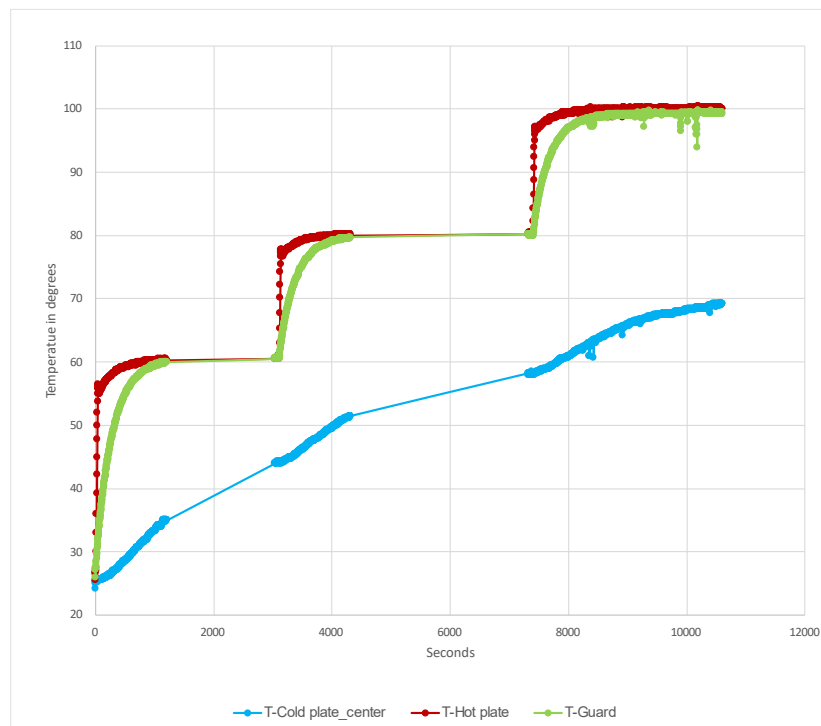
It can be observed that the result closer to the theoretical value of the conductivity is at 80°C of temperature. The mean value of conductivity is 0.28963 while the theoretical value is 0.532. This corresponds to a deviation of 45.55%.

In Tab. 4-3 it can be observed that the difference in percentage between the average of the measurements of both samples is also high. As sample 1 layers are stocked in Z direction the adhesion between layers is greater than in sample 2 where the layers are places one next to the other. The greater the adhesion between layer the greater the conductivity as the results confirm.

Tab. 4-3: Comparison of mean conductivity values of Samples 1 and 2

	λ at T= 60°C	λ at T= 80°C	λ at T= 100°C
Sample 1 (Average)	0.31994	0.37151	0.40638
Sample 2 (Average)	0.26964	0.28963	0.27907
Error in %	15.72%	22.04%	31.33%

In the graph Fig. 4-6 and graph Fig. 4-7 it can be observed that the measurement of the temperature of the guard is not consistent when arriving at values closer to 100°C, which is an indicator of the lack of accuracy of the thermocouples. Moreover, the problem of the disconnection of the machine is repeated for the second experiment, leaving significant periods of time without data recording.

**Fig. 4-6: Measurements Sample 2_1****Fig. 4-7: Measurements Sample 2_2**

4.1.3. Sample 3

In this case, the sample printing direction was parallel to the heat flow direction.

For sample 3 severe errors in the measurement of the temperature of the guard were noticed; see Fig. 4-8. Also, disconnection of the machine occurred.

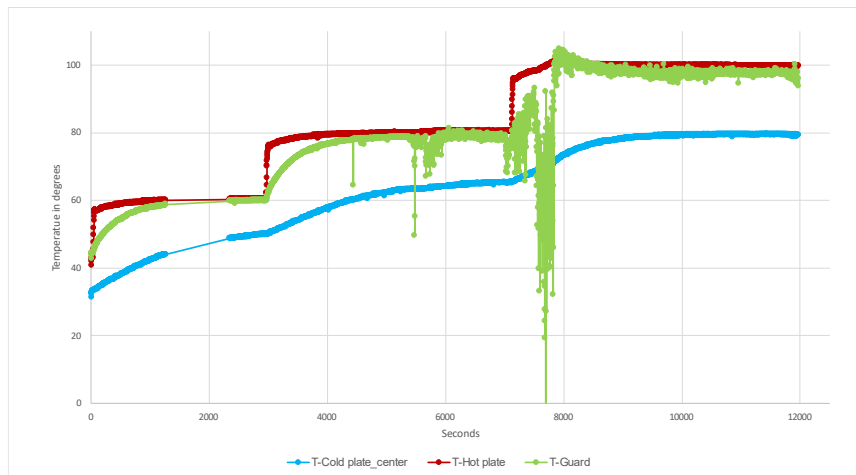


Fig. 4-8: Measurements Sample 3

This sample's conductivity coefficients are found in the following table (Tab. 4-4). In this case, the obtained value of the conductivity coefficient decreases while raising the temperature.

Tab. 4-4: Conductivity coefficient of Sample 3

	λ at T= 60°C	λ at T= 80°C	λ at T= 100°C
Sample 3	0.66970	0.69671	0.58597

4.1.4. Discussion of the conductivity results

As explained in the above subsections, the machine's reliability is not enough to consider the results valid, and for future calculations in this project, the theoretical value of the conductivity will be employed. Moreover, the theoretical value is not equal to the mean of the 3 samples but is closer to the mean.

Table Tab. 4-5 shows that the conductivity coefficient increases when the printing direction is parallel to the heat flow. Sample 3 presents higher conductivity coefficient values than the other two samples printed orthogonal to the heat flow. This assumption will be further investigated in section 4.2.

As stated before, between the samples with orthogonal direction to the heat flow the higher conductivity coefficients are observed in sample 1 because its layers present higher adhesion due to the gravity effects.

Tab. 4-5: Average Conductivity coefficients of all Samples

	λ at T= 60°C	λ at T= 80°C	λ at T= 100°C
Sample 1	0.31994	0.37151	0.40638
Sample 2	0.26964	0.28963	0.27907
Sample 3	0.66970	0.69671	0.58597

4.2. Conduction and fiber alignment

In this chapter, a study of the distribution of the heat flow along the different samples is found. For this purpose, the samples were drilled, and a heat cartridge was added to them. The length data were collected with a thermal camera.

The ratio between the propagation in the X and the Y direction is calculated using the following formula (4-1):

$$C_y = \frac{y_2 - y_1}{x_2 - x_1} \cdot C_x = b \cdot C_x \quad (4-1)$$

In the following calculations, the reference system will be dependent on the flow propagation; the X direction is stated as the direction in which the propagation is the largest.

When the heat cartridge is heated a gradient of temperature with an ellipse shape propagation appears in the sample. For calculating the propagation length an ellipse of the same temperature is selected. The shortest axis represents the Y direction and the X axis the largest. The length is calculated by the subtraction between the final point of the axis minus the starting point in pixels. This procedure is shown in Fig. 4-9.

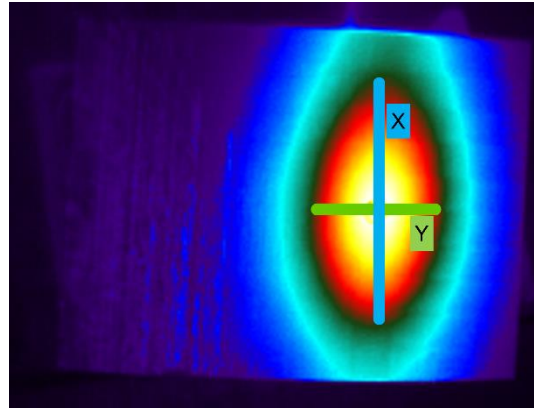


Fig. 4-9: Propagation directions

4.2.1. Heat flow distribution at Sample 1

The heat flow at sample 1 is one and a half times the length in one direction than in the other, as it can be observed in table Tab. 4-6. From this table, it can also be observed that an increase in the temperature decreased the heat flow length in the Y direction with respect to X direction.

Tab. 4-6: Heat flow distribution Sample 1

Temperature in °C of the heat cartridge	x.1	x.2	y.1	y.2	b
75	66	149	231	286	0.663
105	74	142	190	228	0.559

The heat flow propagates more in the printing direction, which explains that there is higher propagation in one direction than in the other (see Fig. 4-10).

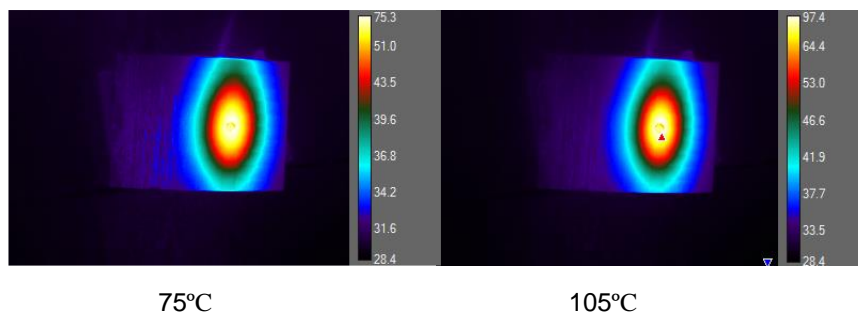


Fig. 4-10: Sample 1 with heat cartridge

4.2.2. Study of the influence of fiber alignment

For this case, different samples whose fiber alignment was known were studied. Even though the voltage and milliamperes applied to the heat cartridge were the same in the four experiments, the value recorded of the heat cartridge varies. This inconvenience can be due to the relocation of the thermocouple every time the experiment was performed.

Tab. 4-7: Heat flow distribution Sample 1

Name of the sample	T in °C	x.1	x.2	y.1	y.2	b	% of fiber alligment
N25	77.00	191	265	89	129	0.541	35.250%
N26	81.57	195	267	89	127	0.528	21.125%
N28	84.02	190	279	98	144	0.517	27.825%
N30	87.96	184	260	100	140	0.526	19.025%

In the table, the data obtained can be observed. The higher the percentage means, the less alignment in the printing direction. The increase of total alignment of the fibers concerning the printing direction in 16% seems not to influence the propagation of the heat flow. As stated in previous sections, the heat flow propagates more in the fiber direction, which explains that there is higher thermal conductivity in the x direction of the samples.

Picture Fig. 4-11 shows how the heat was propagated in the different samples and the temperature distributions. The picture was taken when the heat cartridge reached a steady state.

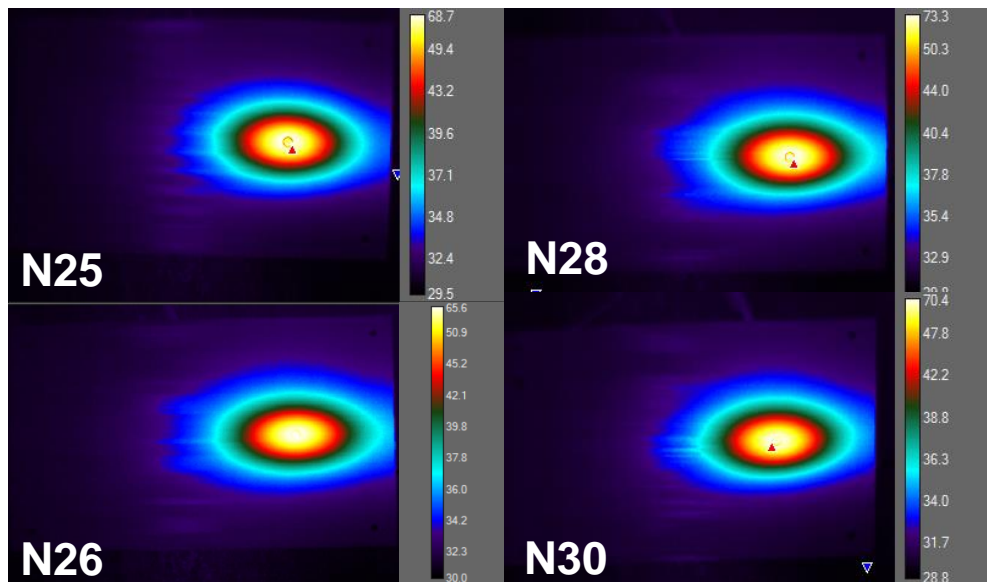


Fig. 4-11: N25, N26, N28, and N30 with heat cartridge

4.3. Convection

In this section a study on the thermal convection coefficient of Sample 1 in three different scenarios is performed.

The surface temperature was measured with a thermal camera, and the maximum temperature value was selected to perform the calculations.

4.3.1. Rough sample

In table Tab. 4-8 the values of the convection coefficient are found, the thickness of the sample, the theoretical value of thermal conductivity, and the different temperature values needed for the calculation.

For the temperature of the surface, the average of the maximum value recorded with the thermal camera during the stationary state is employed.

Tab. 4-8: Convection coefficient Sample 1 rough

Target T in °C	λ	h	d	T hot plate	T surface	T extern
60	0.532	29.0145	0.01043	60.5859	50.2	31.9436
80	0.532	29.3326	0.01043	80.2112	62.7	32.2496
100	0.532	30.4063	0.01043	99.9192	75.5	34.5367

It can be observed that the highest the temperature applied to the sample, the highest the surface temperature. In the first change of temperature of the hot plate for an increase of 20°C, an increase of 12.5°C was present on the surface. In the second rise of temperature for an increase of 20°C at the hot plate, an increase of 12.8 was present on the surface.

As the temperature difference grows while raising the temperature and the ambient temperature recorded is neither constant; the convection coefficient varies between the temperatures, increasing while the temperature increases. The average convection coefficient is 29.5843 W/(m² K).

In the image Fig. 4-12 it can be observed the heat distribution along the sample for the three cases studied. The highest temperatures are usually allocated in the center, however, the effect of reflections interferes with the data obtained with the thermal camera as seen more clearly in the upper left corner of the sample. The difference of surface contact along the sample between the sample and the guard is also noticeable, it results in lower temperatures detected in the upper left corner than in the lower right corner. The increase of the surface temperature when the temperature of the hot plate increases is also noticeable. Finally, the surface presents lines of different temperatures because, in the

parts where the thickness is greater, the temperature drops, in a small percentage, in comparison with the adjacent parts with lower thickness.

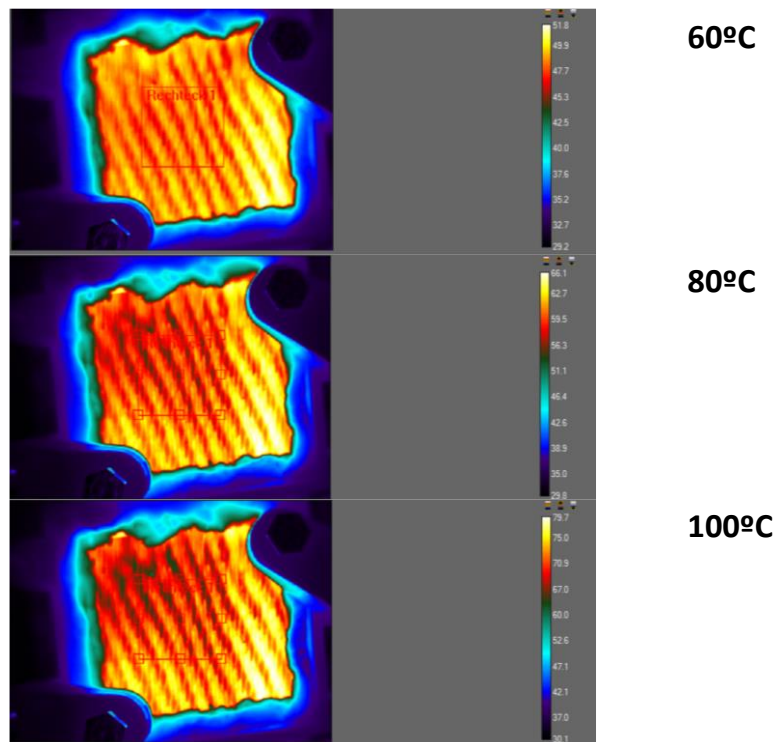


Fig. 4-12: Surface temperature of sample 1 with roughness

4.3.2. Smooth sample

The experiment with the smoothed sample one was performed for a steady state of 80°C. The value of the convection coefficient (see Tab. 4-9) is in the same order of magnitude as in the same sample with the rough surface.

Tab. 4-9: Convection coefficient Sample 1 smooth

Target T in °C	λ	h	d	T hot plate	T surface	T extern
80	0.532	29.0464	0.00996	80.1297	62.8000	30.9323

In the following image, the reflective effects are more noticeable than in the rough surface, as seen in the upper left corner and its temperature drop. It can be seen that there is difference in temperature between the upper left where there is less contact between the surfaces corner and the lower right corner where there is a better contact and therefore

the temperature is higher. As it is a smooth surface, the thickness is constant along the whole sample the gradient of temperatures is smoother with respect to the rough sample.

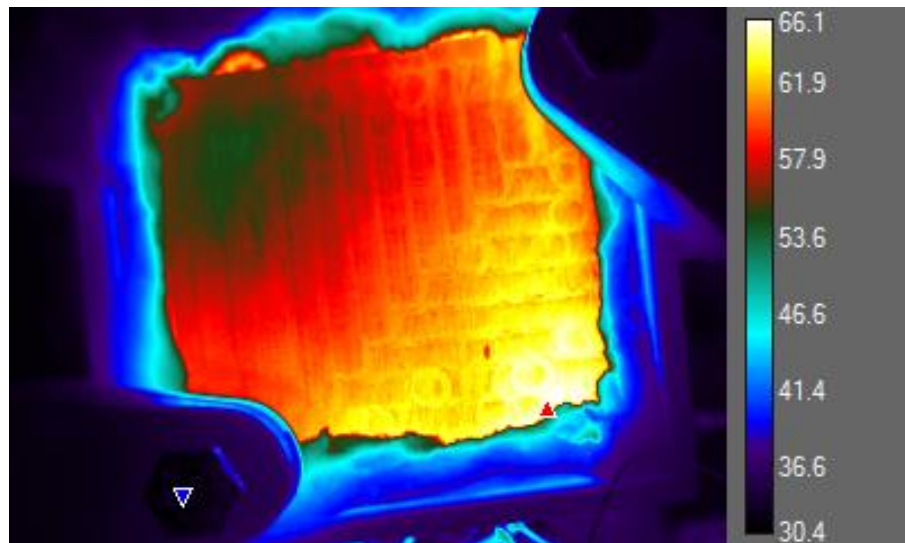


Fig. 4-13: Surface temperature of sample 1 smoothed

4.3.3. Effect of the gravity: rough sample in vertical position

The experiment with the rough sample in a vertical position was performed for a steady state of 80°C. The value of the convection coefficient (see Tab. 4-10) is similar to the two previous samples studied at that temperature.

Tab. 4-10: Convection coefficient Sample 1 rough in vertical position

Target T in °C	λ	h	d	T hot plate	T surface	T extern
80	0.532	29.0850	0.01043	80.1875	61.9500	29.9667

In the following image (Fig. 4-14), the effects of gravity can be appreciated. The hot air is less dense than the cold one due to the highest temperatures are located in the upper part of the sample and the lowest temperatures in the lower part (see the center of the sample). The convection coefficient will be higher at the bottom of the sample as the

temperature of the surface decreases here. Reflection effects appear at the sides of the sample.

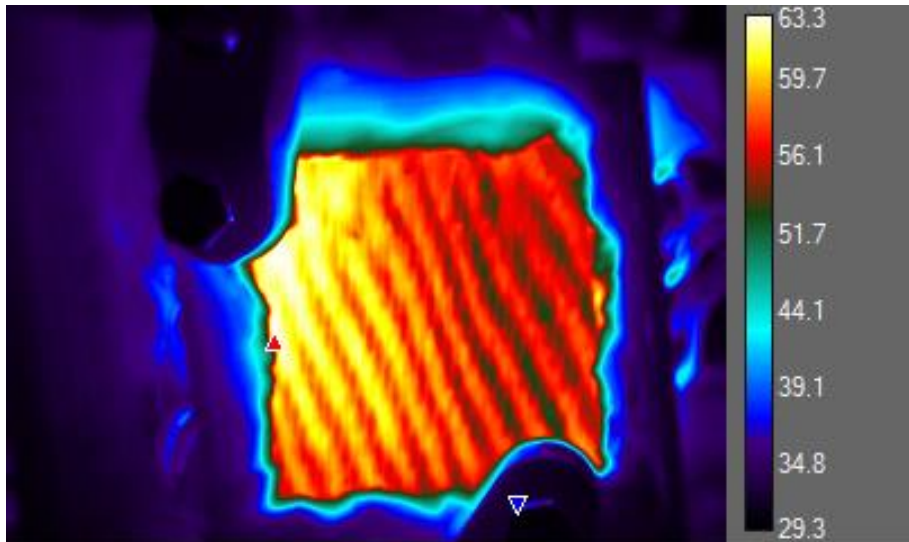


Fig. 4-14: Surface temperature of sample 1 with roughness in vertical position

In summary the table Tab. 4-11 shows all the acquired convection coefficients are shown, as stated before the values corresponding to a target temperature of 80°C are similar in the three cases.

Tab. 4-11: Convection coefficient of the 3 experiments

Sample	Target T in °C	h
Rough surface	60	29.0145
Rough surface	80	29.3326
Rough surface	100	30.4063
Smooth surface	80	29.0464
Rough surface in vertical position	80	29.0850

5. Summary and outlook

A study of the conductivity and convection coefficients and the propagation of the heat flow along a CFRP composed of 20% of short carbon fibers was developed.

As a general conclusion for the conductivity coefficient, it has been verified that the conductivity coefficient of a carbon composite material increases when the printing direction is parallel to the heat flow. In other words, the thermal conductivity will decrease when the printing direction is orthogonal to the heat source. It has also been verified that the higher the adhesion between layers the higher the conductivity of the composite.

The experiments showed that the results were not accurate even though some conclusions were obtained from them. For more accurate results, other approaches such as laser-flash diffusivity are recommended.

For future studies with the same machine employing the guarded heat method, it is recommended to change or at least review the thermocouples. It is advised to perform the experiment in a room with constant room temperature and without machines working nearby that could imply an exchange of heat, such as refrigerators. For better results, it is recommended to check that the correct pressure is applied to the cold plate; wood sticks that present a low thermal conductivity can be used under the bottom of the screw if there is a gap between the screw and the cold plate.

The heat cartridge experiment showed, that there was no correlation or at least a minor correlation between the conductivity and the alignment of the fibers with the printing direction. More alignment on the fibers in the printing direction in the ranges studied in this project, increase of 16% of total fiber alignment, didn't imply a significant difference between the magnitudes of the direction of propagation.

Moreover, the experiment also verified that the conductivity increased in the printing direction as the expansion of the heat had an oval shape and not a circular shape.

The heat cartridge experiment could be improved with the setup of a test bench that avoided the problems of the collocation of the thermocouple on the heat cartridge.

Finally, for the convection coefficient experiment, multiple effects were observed.

The temperature gradient of the surface has a less drastic change in temperature on the smooth surface rather than on the rough surface. Reflection effects that appeared on the thermal camera images increased when the sample's surface was smooth. To avoid this problem, different places to set the thermal camera should be studied to choose the one with less external influence on the images.

In the rough surface case, the thermal camera detected the difference in temperature created by the increase or decrease of thickness due to the roughness.

For the vertical plate, the highest surface temperature values were on the top of the sample because of gravity. That's to say that the convection coefficient will be higher at the bottom of the sample. Nevertheless, this difference in the convection coefficient can be neglected for the studied sample length.

To conclude, the CFRP studied is suitable for manufacturing autoclave tools for aircraft flaps in terms of thermal properties as it can resist the high process temperatures occurring during manufacturing. A more efficient additive manufacturing process can be achieved in producing this composite material, as its thermal properties are now known.

REFERENCES

- [1] Campbell FC. Structural composite materials. Materials Park Ohio: ASM International; 2010.
- [2] Mohamed Sahbi Loukil. Experimental and Numerical Studies of Intralaminar Cracking in High Performance Composites: Scientific Figure on ResearchGate; Available from: https://www.researchgate.net/figure/Composite-structure-content-on-the-Boeing-787-1_fig3_324436953.
- [3] Lepoivre A, Boyard N, Levy A, Sobotka V. Heat Transfer and Adhesion Study for the FFF Additive Manufacturing Process. *Procedia Manufacturing* 2020;47:948–55.
- [4] Ivey M, Melenka GW, Carey JP, Ayranci C. Characterizing short-fiber-reinforced composites produced using additive manufacturing. *Advanced Manufacturing: Polymer & Composites Science* 2017;3(3):81–91.
- [5] Barbero EJ. Introduction to composite materials design. Boca Raton: Taylor & Francis CRC Press; 2018.
- [6] Barbero EJ. Introduction to Composite Materials Design, Third Edition. Boca Raton, FL: CRC Press; 2017.
- [7] Kern. <https://www.kern.de/de/technisches-Datenblatt-polyetherimid>; Available from: https://www.kern.de/de/technisches-datenblatt/polyetherimid-pei?n=2501_1.
- [8] J. Carvill. Mechanical Engineer's Data Handbook: Butterworth-Heinemann; 1994.
- [9] Singh S, Ramakrishna S, Berto F. 3D Printing of polymer composites: A short review. *Mat Design & Process Comms* 2020;2(2).
- [10] Attaran M. The rise of 3-D printing: The advantages of additive manufacturing over traditional manufacturing.: Business Horizons; 2017.
- [11] Wang X, Jiang M, Zhou Z, Gou J, Hui D. 3D printing of polymer matrix composites: A review and prospective.: *Composites Part B: Engineering*; 2017.

-
- [12] Hmeidat NS, Elkins DS, Peter HR, Kumar V, Compton BG. Processing and mechanical characterization of short carbon fiber-reinforced epoxy composites for material extrusion additive manufacturing. *Composites Part B: Engineering* 2021;223:109122.
- [13] Iowa State University. Materials and Processes: Thermal Conductivity; Available from: https://www.nde-ed.org/Physics/Materials/Physical_Chemical/ThermalConductivity.xhtml.
- [14] Mutnuri B. Thermal conductivity characterization of composite materials. Graduate Theses, Dissertations, and Problem Reports. Morgantown, West Virginia, USA; 2006.
- [15] ASM Handbook (ed.). Volume 21, Composites; 2001.
- [16] Mirmira SR. Thermal conductivity of fibrous composites: experimental and analytical study. Ph D Dissertation. USA; 1999.
- [17] Ibrahim Y, Elkholy A, Schofield JS, Melenka GW, Kempers R. Effective thermal conductivity of 3D-printed continuous fiber polymer composites. *Advanced Manufacturing: Polymer & Composites Science* 2020;6(1):17–28.
- [18] Tritt TM (ed.). Thermal conductivity: Theory, properties, and applications. New York, NY, Boston, Dordrecht, London, Moscow: Kluwer Academic/Plenum Publishers; 2004.
- [19] Grünfelder M. Test bench for determining the thermal properties of additively manufactured fiber composites. Semesterarbeit. München, Bayern, Germany.
- [20] Bejan A. Convection Heat Transfer. 4th ed.: John Wiley & Sons; 2013.
- [21] Moreira TA, Colmanetti ARA, Tibiriçá CB. Heat transfer coefficient: a review of measurement techniques. *J Braz. Soc. Mech. Sci. Eng.* 2019;41(6).
- [22] Wilson EE. A basis of rational design of heat transfer apparatus; 1915.
- [23] Fernandez-Seara J, Uhía FJ, Sieres J, Campo A. A general review of the Wilson plot method and its modifications to determine convection coefficients in heat exchange devices; 2007.
- [24] Colburn AP. A method of correlating forced convection heat transfer data and a comparison with fluid friction; 1964.

- [25] Goldstein RJ CHH. A review of mass transfer measurements using naphtalene sublimation; 1995.

LIST OF FIGURES

Fig. 1-1: " Composite structure content on the Boeing 787 [2]"	1
Fig. 2-1: "Production processes of composites adapted from [1]"	7
Fig. 2-2: Guarded heat flow mechanism	13
Fig. 3-1: Material extrusion.....	19
Fig. 3-2: Cutting machine.....	20
Fig. 3-3: Drilling process	20
Fig. 3-4: Guarded heat flow meter at the TUM Chair of Carbon Composites.....	21
Fig. 3-5: PEI Airtech 1350 samples printing direction	22
Fig. 3-6: Convection measurement	23
Fig. 3-7: Test bench for convection measurements.....	25
Fig. 4-1: PEI Airtech 1350 samples printing direction	27
Fig. 4-2: Measurements Sample 1_1	29
Fig. 4-3: Measurements Sample 1_2.....	29
Fig. 4-4: Measurements Sample 1_3.....	30
Fig. 4-5: Measurements Sample 1_0.....	31
Fig. 4-6: Measurements Sample 2_1	33
Fig. 4-7: Measurements Sample 2_2.....	33
Fig. 4-8: Measurements Sample 3.....	34
Fig. 4-9: Propagation directions	36
Fig. 4-10: Sample 1 with heat cartridge	37
Fig. 4-11: N25, N26, N28, and N30 with heat cartridge.....	38
Fig. 4-12: Surface temperature of sample 1 with roughness	40
Fig. 4-13: Surface temperature of sample 1 smoothed.....	41
Fig. 4-14: Surface temperature of sample 1 with roughness in vertical position.....	42

LIST OF TABLES

Tab. 2-1: Matrix and fiber properties [7,8]	5
Tab. 2-2: Direct method convection techniques [21]	16
Tab. 4-1: Conductivity coefficient of Sample 1, average and variance.....	28
Tab. 4-2: Conductivity coefficient of Sample 2, average and variance.....	31
Tab. 4-3: Comparison of mean conductivity values of Samples 1 and 2	32
Tab. 4-4: Conductivity coefficient of Sample 3.....	34
Tab. 4-5: Average Conductivity coefficients of all Samples.....	35
Tab. 4-6: Heat flow distribution Sample 1	36
Tab. 4-7: Heat flow distribution Sample 1	37
Tab. 4-8: Convection coefficient Sample 1 rough.....	39
Tab. 4-9: Convection coefficient Sample 1 smooth	40
Tab. 4-10: Convection coefficient Sample 1 rough in vertical position.....	41
Tab. 4-11: Convection coefficient of the 3 experiments	42

